Cellular Signalling 97 (2022) 110372

Contents lists available at ScienceDirect

Cellular Signalling

journal homepage: www.elsevier.com/locate/cellsig

Suppression of COX-2/PGE_2 levels by carbazole-linked triazoles *via* modulating methylglyoxal-AGEs and glucose-AGEs – induced ROS/NF-κB signaling in monocytes

Humera Jahan [a,**], Nimra Naz Siddiqui [a], Shazia Iqbal [b], Fatima Z. Basha [b], Sadia Shaikh [a], Marina Pizzi [d], M. Iqbal Choudhary [a,b,c,*]

[a] Dr. Panjwani Center for Molecular Medicine and Drug Research, International Center for Chemical and Biological Science, University of Karachi, Karachi 75270, Pakistan
[b] H.E.J. Research Institute of Chemistry, International Center for Chemical and Biological Science, University of Karachi, Karachi 75270, Pakistan
[c] Department of Chemistry, Faculty of Science and Technology, Universitas Airlangga, Komplek Kampus C, Jl. Mulyorejo, Surabaya 60115, Indonesia
[d] Department of Molecular and Translational Medicine, University of Brescia, Brescia 25123, Italy

ARTICLE INFO

Keywords:
Diabetes
Advanced glycation end products
Atherosclerosis
Cyclooxygenase-2
Monocytes
Protein glycation

ABSTRACT

Chronic hyperglycemia favours the formation of advanced glycation end products (AGEs) which are responsible of many diabetic vascular complications. Keeping in view the medicinal properties of the1,2,3-triazole-conjugated analogs, the present study was designed to evaluate the possible effect of carbazole-linked 1,2,3-triazoles **2–16** against glucose- and methylglyoxal-AGEs-induced inflammation in human THP-1 monocytes. *In vitro* antiglycation, and metabolic assays were used to determine antiglycation, and cytotoxicity activities. DCFH-DA, immunostaining, immunoblotting, and ELISA techniques were employed to study the ROS and levels of proinflammatory mediators in THP-1 monocytes. Among all the synthesized carbazole-linked 1,2,3 triazoles, compounds **2**, **7**, **8**, and **11–16** showed antiglycation activity in glucose- and MGO-modified bovine serum albumin models, whereas parent compound **1** only exhibited activity in glucose-BSA model. The metabolic assay demonstrated the non-toxic profile of compounds **1–2**, **11–13**, and **15** up to 100 μM concentration in both HepG2 and THP-1 cell lines. We found that compounds **11–13**, and **15** attenuated AGEs-induced ROS formation ($P < 0.001$), and halted NF-κB translocation ($P < 0.001$), likewise standard drugs, PDTC, rutin, and quercetin, in THP-1 monocytes. Among the derivatives, compounds **12**, and **13** also suppressed the AGEs-induced elevation of COX-2 ($P < 0.001$) and PGE_2 ($P < 0.001$). Our data show that the carbazole-linked triazoles **12**, and **13** hampering the formation of glycation products, prevent the activation of AGEs-ROS-NF-κB signaling pathway, and limit the proinflammatory COX-2 protein, and PGE_2 induction in human THP-1 monocytes. Both these compounds can thus serve as leads for further studies towards the treatment and prevention of diabetic vascular complications.

1. Introduction

Hyperglycemia is the leading cause of progression of cardiovascular impairments in diabetes. These include micro- and macro-vascular complications, such as coronary artery disease, peripheral artery disease, nephropathy, neuropathy, retinopathy, and others. This may lead to organ failure or even death [1–3]. Studies conducted on *in vivo* animal models suggested the putative role of hyperglycemia in the development of atherosclerosis (ATH). Hyperglycemia associated pathogenic factors that include the formation of advanced glycation end products (AGEs) play a key role in the on-set and progression of ATH in diabetics [4–6]. AGEs are formed as a result of non-enzymatic glycation of proteins, also known as Millard reaction, which lead to the modification in their structures and functions [6]. During AGEs formation, the fragments of Schiff base increase the reactive dicarbonyl intermediates production; glyoxal (GO) and methylglyoxal (MGO). These highly reactive moieties

* Corresponding author at: H.E.J. Research Institute of Chemistry, International Center for Chemical and Biological Science, University of Karachi, Karachi 75270, Pakistan.
** Corresponding author at: Dr. Pajwani Center for Molecular Medicine and Drug Research, International Center for Chemical and Biological Sciences, University of Karachi, Karachi 75270, Pakistan.
E-mail addresses: humerajahan@iccs.edu, jahan_pcmd@yahoo.com (H. Jahan), iqbal.choudhary@iccs.edu (M.I. Choudhary).

https://doi.org/10.1016/j.cellsig.2022.110372
Received 7 April 2022; Received in revised form 24 May 2022; Accepted 25 May 2022
Available online 29 May 2022
0898-6568/© 2022 Published by Elsevier Inc.

trigger protein glycation reaction at a much faster rate than the precursor sugars (glucose, fructose, and ribose) [4,7]. The resulting AGEs promote vasculitis and atheroma formation in diabetic patients [8].

Earlier studies have found that AGEs ligation with their receptor, RAGE (receptor for AGEs), on blood monocytes causes intracellular oxidative stress, with subsequent upregulation of nuclear factor κB (NF-κB), and hence trigger inflammatory cascades [9,10]. It results in increased levels of various proinflammatory genes, including cyclooxygenase-2 (COX-2), tumor necrosis factor- α (TNF-α), interleukin- β (IL-1β), interleukin- 6 (IL-6) [1,11–14]. COX-2 is associated with increased levels of pro-inflammatory signaling mediator prostaglandin E_2 (PGE_2) in blood monocytes [15] (Fig. 1). It has been found that COX-2 induction, and increased PGE_2 levels are risk factors for atherosclerotic plaque development in low-density lipoprotein (LDL) receptor-deficient mice. PGE_2 interacts with cell surface scavenging receptors, expressed on blood monocytes, and causes uptake of LDL to form fatty streak, and atheroma formation [16].

Animal models of atherosclerosis, genetic or induced, revealed remarkable beneficial effects with the treatment of nonsteroidal anti-inflammatory drugs (NSAID) [17–19]. Individuals on routine treatment with aspirin or NSAIDs have 40–50% reduced risk of developing cardiovascular diseases. Thus, although many commercially available drugs, including rofecoxib, valdecoxib, etodolac, celecoxib, etoricoxib, nimesulide, diclofenac, and indomethacin, have shown to inhibit COX-2 enzyme activity in *ex vivo* assays of prostaglandin formation in whole blood, and the inhibitory activity of these drugs was only 50% [20].

Several studies have been conducted to identify the inhibitors of the glycation process. So far, various glycation inhibitors, including pyridoxamine, metformin, kremezin, *N*-phenacylthiazolium bromide (cross-link breaker), OPB-9195 (carbonyl amine blocker), alagebrium, atorvastatin, and guanidines, have been identified to interfere with different stages of the Millard reaction [21,22]. Aminoguanidine, a prototype of glycation inhibitor, was found to reduce AGEs-induced diabetopathies *via* inhibiting conversion of highly reactive dicarbonyl compounds to AGEs, as well as formation of cross-links and free radical species [23,24]. However, it was not approved for clinical use due to adverse effects, such as vasculitis, gastrointestinal and liver impairment, antinuclear antibody development, pernicious-like anemia, and neoplastic tumors in pancreas and kidney [25]. Besides, other inhibitors were also not attained much acceptance in clinical settings because of adverse effect and/or reduced potency. Therefore, there is a need to identify effective and safe protein glycation inhibitors to prevent chronic inflammation, organs damage, and death in diabetic patients. Our research group has initially identified 2, 4-dinitroanilino - benzoic acid as a promising insulinotropic agent that helps control glycemic index in diabetic rats [7]. Anthranilic acid derivatives have also shown to inhibit the AGEs formation in hepatocyte model, *i.e.*, the cells of the major glucose regulating and detoxifying organ [7]. Besides, we have also reported that gliclazide alters macrophage polarization in diabetic atherosclerosis [26]. We continued to work on the identification of novel agents able to limit AGE-RAGE-mediated inflammatory pathways.

Over the last few decades, 9*H*-carbazole and triazole moieties have attracted much attention in medicinal chemistry due to their wide range of biological activities. The carbazole scaffold shows activities against bacteria, cancer, and Alzheimer's disease [27]. Whereas, triazole nucleus prevents disorders by ligation with proteins, such as enzymes and cellular receptors [28]. Currently, 1,2,3-triazole-conjugated analogs are the focus of attention in medicinal chemistry. They are successfully being used drug candidates, such as fluconazole, itraconazole, voriconazole, posaconazole, a *etc.* [29].

Keeping in view a high prevalence of vascular complications in diabetes, and involvement of AGEs as a key pathogenic factor, the current study was designed to investigate the potential of carbazole-linked 1,2,3-triazoles as antiglycating agents. We hypothesized that carbazole-linked 1,2,3-triazole analogs can inhibit the AGEs formation and associated inflammatory cascade in *in vitro* diabetic environment, and thus

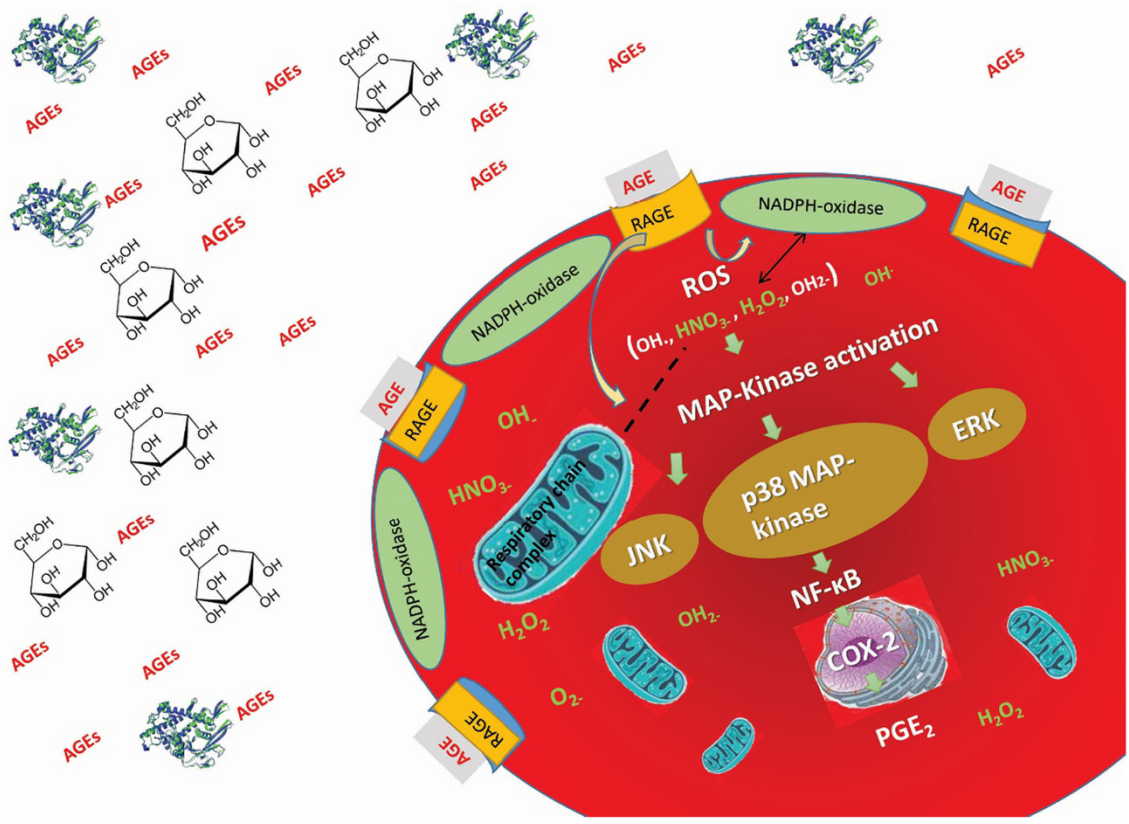

Fig. 1. AGE-RAGE induce intracellular inflammatory cascade.

can prevent / or delay the onset of cardiovascular complications in diabetes. Therefore, we evaluate the potential of carbazole-linked 1,2,3-triazole analogs against the AGEs formation, and to prevent the signaling mechanism of AGE-RAGE-mediated ROS-dependent NF-κB-induced COX-2 upregulation and associated PGE_2 production. In the present study, we employed the human blood monocytes model, i.e. THP-1 cells, to study the RAGE-ligation mediated upregulation of proinflammatory cytokines signaling in hyperglycemic milieu [22,30–32]. In contrast to lipopolysaccharide (LPS) model or tissue macrophage system, the treatment of human monocytes with reducing sugar (glucose) or dicarbonyl sugar (methylglyoxal) provides an excellent model of diabetic pathological conditions to study the inflammatory cascade. Hence, we employed this model to identify the potential of carbazole-linked 1,2,3-triazoles analogs in RAGE-ligation mediated COX-2 protein/PGE_2 inflammatory cytokine up-regulation [32]. To our knowledge, this is the first study examining the antiglycation activity of carbazole-linked 1,2,3-triazoles and their role in preventing AGE-mediated up-regulation of COX-2 protein and PGE_2 formation.

2. Methodology

2.1. In vitro antiglycation activity of carbazole-linked 1,2,3 triazoles analogs

Carbazole, and carbazole-linked 1,2,3-triazoles analogs were tested for their antiglycation activity in two different models: glucose- and MGO-modified BSA models. Rutin and quercetin (Sigma-Aldrich Chemical Corporation, USA) were used as reference compounds, as they are known to ameliorate glycation in the previously reported studies. The antiglycation activity were performed as per the described protocol of Jahan, *et al* [33]. Briefly, at first, in a 96-well black fluorescent plate, 10 mg/mL of bovine serum albumin (BSA; Thermo Fisher Scientific, USA), 0.5 M of glucose (Scharlau, Spain), or 0.1 M of MGO (Sigma-Aldrich USA) were added, and incubated for 7- and 1-day in the glucose and MGO models, respectively, at 37 °C in a 0.1 M sodium phosphate buffer. The buffer contained 0.1 mM sodium azide to prevent microbial growth. Prior to incubation, all the compounds were solubilized at 1 mM concentration in 10% of DMSO, and were added to the reaction mixture in a plate.

After the incubation period, fluorescence intensity of glucose- and MGO-modified BSA were measured at 340*exc*-440*emi* nm for glucose, and 355*exc*-460*emi* nm for MGO. The percent inhibition was quantified by the following formula:

$$\%\text{Inhibition of fluorescence} = (1 - \text{Fluorescence of test compounds}/\text{Fluorescence of glycated BSA}) \text{ x } 100$$

Compounds those exhibited greater than 50% inhibition were diluted serially to measure half-maximal inhibitory concentration (IC_{50}), using EZ-FIT enzyme kinetics software [34,35].

2.2. Human monocyte and hepatocyte culture

Human THP-1 monocytes (European Collection of Authenticated Cell Cultures (ECACC), Sigma-Aldrich, USA) and HepG2 (human hepatocytes) (American Type Tissue Culture Collection (ATCC), USA) were maintained as per the described protocols of Balakrishna., *et al*, and Jiang., *et al.* with slight modifications [36,37]. Briefly, the monocytes and hepatocytes were grown in tissue culture 75 cc flask containing ATTC modified RPMI 1640 medium (Gibco, Thermo Fisher Scientific, USA), and minimum essential medium (MEM, Gibco, Thermo Fisher Scientific, USA), respectively. 10% Fetal bovine serum (Gibco, Thermo Fisher Scientific, USA) was used for both cell lines. Controlled atmosphere containing 5% CO_2 to become 80–90% confluent was thus provided. The passage numbers were carefully monitored, until they reached 20.

The cells morphology was observed by using an inverted microscope (Nikon E200, Japan). All the chemicals and compounds, used to study the intracellular cascade, were diluted with the same assay medium.

2.3. Cellular toxicity

Cellular toxicity of carbazole and identified lead carbazole-linked 1,2,3-triazoles analogs in glucose- and MGO-mediated protein glycation assays were analyzed at various concentrations (10, 30, 50, 100, 200, and 500 μM) for their toxicity profile, using HepG2, and THP-1 cell lines. The MTT, and WST-1 metabolic assay were performed for HepG2, and THP monocytes. Briefly, 7×10^4 of HepG2 cells/mL, and 20×10^4 of THP-1 monocytes/mL were seeded in 96-well sterile cell culture treated plates, and treated with the compounds for 24 h. Followed by the incubation, MTT (20 μL), and WST-1 (20 μL) reagents were added to each well of HepG2 cells, and THP-1 monocytes, respectively. After 4 h of incubation, the medium was carefully aspirated. The DMSO (100 μL) were used to solubilize formazan crystals in MTT-treated HepG2 cells. The metabolic activity was initiated by cleavage of tetrazolium salt (MTT, and WST-1) to produce formazan in viable cells by the action of mitochondrial dehydrogenases. The colorimetric measurement was performed at 540, and 450 nm, respectively, using a microplate reader (Varioskanmicroplate reader, Thermo Fisher Scientific, USA). The cells without any treatment have served as negative control, while cells treated with doxorubicin have served as positive control.

2.4. Glucose- and MGO-derived AGEs formation

The monocytes were stimulated by the exposure of glucose- and MGO-derived AGEs (MGO-AGEs). The preparation of glucose-AGEs was done by incubating fatty acid-free BSA (10 mg/mL, Calbiochem, Merck, Germany) with glucose (500 mM), D-fructose (50 mM, Scharlau, Spain), and MGO (3 mM) in PBS (100 mM; pH = 7.4) medium at 60 °C for 6 weeks in a dark, and sterile condition [38]. Whereas MGO-AGEs were formed by slightly modifying the method of Shanmugam *et al* [22]. Briefly, fatty acid-free BSA (50 mg/mL) was incubated with MGO (500 mM) for 24 h under sterile conditions. The ionization power was critically controlled during the complete incubation period, and maintained to 7.4 pH by using sodium hydroxide (NaOH; 1 M). Subsequently, the prepared mixtures were dialyzed against PBS to remove free unbound glucose, and MGO. The fluorometric measurement (Varioskanmicroplate reader, Thermo Fisher Scientific, USA), and estimation of endotoxins levels (Lonza, Chromogenic LAL Assay Kit, Thermo Fisher Scientific, USA) were carried out prior to use. Both the AGEs mixtures were aliquoted in sterile vials to avoid the freeze-thaw cycles, and stored at −80 °C till use.

2.5. Antioxidant property analysis via H2DCFDA assay

2′,7′-Dichlorodihydrofluorescein diacetate (H_2DCF-DA) was used to evaluate the ROS generation in THP-1 monocytes, according to the method described by Hu, Y., *et al.* with minor modifications [39]. The H_2DCF-DA is a non-fluorescent permeant probe that upon cleavage by intracellular esterases becomes impermeant. Upon oxidation by intracellular ROS, it generates fluorescent DCF [40]. Briefly, THP-1

monocytes (1×10^6 cells/mL) were seeded in a 96-well black fluorescent plate, and pre-treated with H_2DCF-DA (10 μM; Sigma-Aldrich, USA) for 45 min at 37 °C in a dark. Followed by washing with phenol red free modified RPMI to prevent false results, cells were exposed with potent antiglycating analogs with non-toxic profile for an hour at 37 °C in a 5% CO_2 incubator. Standard antiglycating compounds: rutin and quercetin, were used to compare the activity of active carbazole-linked 1,2,3-triazoles analogs [41]. While pyrrolidine dithiocarbamate (PDTC), an kβ inhibitor, was used as a standard. All the compounds were used in varying concentrations (10, 30, 50, and 100 μM). Following the treatment with compounds, monocytes were stimulated to produce ROS by using 50 μg/mL AGEs (glucose- and MGO-AGEs) for 24 h. H_2O_2 (10 μM), and AGEs were used as positive controls, while BSA-treated monocytes have served as a negative control.

Fluorescence was measured at 485exc-520emi nm, using spectrofluorometer (Varioskanmicroplate reader, Thermo Fisher Scientific, USA).

2.6. NF-κB nuclear translocation analysis via immunochemistry

To detect nuclear translocation of NF-κB p65 subunit in human THP-1 monocytes, immunocytochemistry technique was employed. Monocytes (1×10^6 cells/mL) were pre-treated with 100 μM of selected analogs for one hour, as this concentration exhibited a maximum inhibition in AGE_S-mediated ROS generation was observed. Subsequently, monocytes were exposed to AGEs (50 μg/mL) (glucose- and MGO-AGEs) for one hour at 37 °C. Later, cells were washed thrice with chilled PBS, fixed and permeabilized by paraformaldehyde (4%; 10 min) and triton X-100 (0.2%; 10 min), respectively. To prevent the nonspecific binding, the permeabilized monocytes were treated with blocking solution (1% BSA dissolved in PBS and Tween-20 (0.1%)) for an hour at room temperature. These monocytes were then incubated with NF-κB p65 (primary antibody, 1:300, Thermo Fisher Scientific, USA) overnight at 4 °C, and then with Fluorescein isothiocyanate (FITC)-conjugated polyclonal antibody to rabbit IgG (secondary antibody, 1:1000 Abcam, UK). The nucleus of monocytes was counterstain with DAPI (Thermo Fisher Scientific, USA). The cells, treated with 50 μg/mL of BSA, and AGEs, have served as negative- and positive controls, respectively. All the images were taken by Nikon 90i microscope, fixed with DXM-1200 digital camera (Nikon, Japan). ImageJ (Image processing and analysis Java program- NIH) was used for quantitative analysis of mean p65 fluorescence intensity with mean fluorescence of DAPI positive monocytes in a six-random high-power field for each treatment.

2.7. Proinflammatory enzyme COX-2 analysis via immunoblotting

The immunoblotting was performed to identify the levels of COX-2 enzyme, and ß-actin protein in human THP-1 monocytes. The cells were pretreated with analogs (100 μM) for one hour, and then incubated with 50 μg/mL of AGEs (glucose- or MGO-AGEs) for 6 h. To lyse the monocytes, RIPA lysis buffer was used, and sonication was performed. Later, monocytes were subjected to centrifugation at 12,000 rpm at 4 °C for 20 min. The lysate was aliquoted, and stored at −20 °C till analysis.

10% gel (SDS-PAGE) was run to separate the 50 μg/mL of COX-2 enzyme, and β-actin protein bands. The bands were transferred to nitrocellulose membrane, and membrane was incubated with a blocking solution for one hour at room temperature to prevent it from nonspecific binding. After that membranes were incubated with monoclonal COX-2 (Thermo Fisher Scientific, USA) and β-actin (Cloud-Clone Corp., China) primary antibodies for 24 h at 4 °C to probe the protein bands. The membrane was washed with tris buffer saline tween (TBST), and incubated with HRP mouse mono anti-rabbit IgG (secondary antibody; Abcam, UK) at room temperature for one hour. To visualize the bands, chemiluminescence detection kit (ECL) (Sangon Biotech, China) was used, and densitometric analysis was performed by using ImageJ (Image processing and analysis in Java - NIH).

2.8. Pro-inflammatory cytokine PGE_2 analysis via ELISA

Briefly, THP-1 monocytes (5×10^5 cells/mL) were plated in a 6-well cell-culture treated plate to pre-expose with analogs (100 μM) for one hour, and then activated with 50 μg/mL of AGEs for 6 h. The cells were centrifuged at 1000 rpm for 10 min, pallets were discarded, and the levels of PGE_2 in supernatant were measured by using the commercially available PGE_2 competitive ELISA kit (Cloud-Clone Corp., China), in accordance to the manufacturer's protocol.

2.9. Statistical analysis

All the statistical analysis was conducted using IBM SPSS (Statistical Package for the Social Sciences) version 21.0. The quantitative data were represented as means ± standard deviation (SD) of three to five *in vitro* cellular model-based experiments. The significance among variables of various mechanistic activities at various concentrations of analogs were compared with glucose- and MGO-AGEs (positive control) and quercetin, rutin, and PDTC (standards) by applying one-way analysis of variance (ANOVA). Followed by *post hoc* Tukey Alpha test analysis, and *P*-value ≤ 0.05 was considered statistically significant.

3. Results

3.1. Inhibition of protein glycation via carbazole- linked 1,2,3-triazoles

In the present study, the conjugated carbazole-1,2,3-triazoles compounds (Fig. 2) **2–16** were initially tested to examine their inhibitory potential against *in vitro* glucose- and MGO-induced non-enzymatic BSA-glycation. Our data revealed that the parent molecule carbazole (compound **1**) exhibit a weak inhibition (IC_{50} 763.3 ± 15.2 μM) against glucose-modified BSA, while was found inactive in MGO-modified BSA model. The presence of triazole nucleus with carbazole moiety (compound **2**) dramatically increased the inhibitory potential by showing IC_{50} 351.3 ± 7.09 μM, and 797 ± 7.0 μM in glucose- and MGO-BSA models, respectively.

To compare the antiglycation potential of carbazole-triazole derivatives, selected flavonoids rutin and quercetin, were selected as reference molecules. The skeleton of these molecules carries polyhydroxy moieties serving as free radical scavengers in non-enzymatic glycation reaction [42]. They found to have various medicinal properties, including anticancer, anti-inflammatory, and antiaging activities [32]. Among the tested flavonoids, we found that rutin has relatively higher antiglycation potential in both models (glucose-BSA: $IC_{50} = 83 \pm 1.0$ μM, and MGO-BSA: 104 ± 2.0 μM), as compared to quercetin (glucose-BSA: $IC_{50} = 96 \pm 4.0$ μM, and MGO-BSA: 138 ± 4.4 μM). These results on rutin and quercetin were consistent with previous data [42].

To study the antiglycation activity of carbazole-linked 1,2,3-triazoles derivatives, the compounds **3–12** having substitutions on aryl, such as X (F, Cl, Br, I) Me, OMe, and NO_2 groups, compounds **13**, and **14** bearing nitrogen heterocycles (pyridyl, imidazolyl), and compounds **15**, and **16** (dimers of carbazole triazole) were tested. The four halogenated congeners *i.e.,* compounds **3–6** carrying fluoro, chloro, bromo, and iodo substitution at the C-3 position, were found to be inactive in both glycation models.

Methylation at the C-2 (compound **7**) has resulted in a moderate inhibition in glucose-BSA ($IC_{50} = 180.3 \pm 1.52$ μM) and MGO-BSA (IC_{50} = 275 ± 5.0 μM) models, as compared to reference molecules. To explore the optimal carbon position for methyl substitution, a regioisomer of compound **7,** *i.e.,* compound **8,** was tested for antiglycation activity. Compound **8** carrying a methyl group at the C-3 position, revealed a remarkable higher inhibitory activity against glucose- and MGO-BSA as showed by the reduced IC_{50} (glucose-BSA: $IC_{50} = 65 \pm 10.0$ μM, MGO-BSA: IC_{50} 130 ± 5.0 μM). Furthermore, it showed a greater activity than the reference quercetin in both models, while rutin only revealed inhibition in glucose-BSA model. On the other hand, the

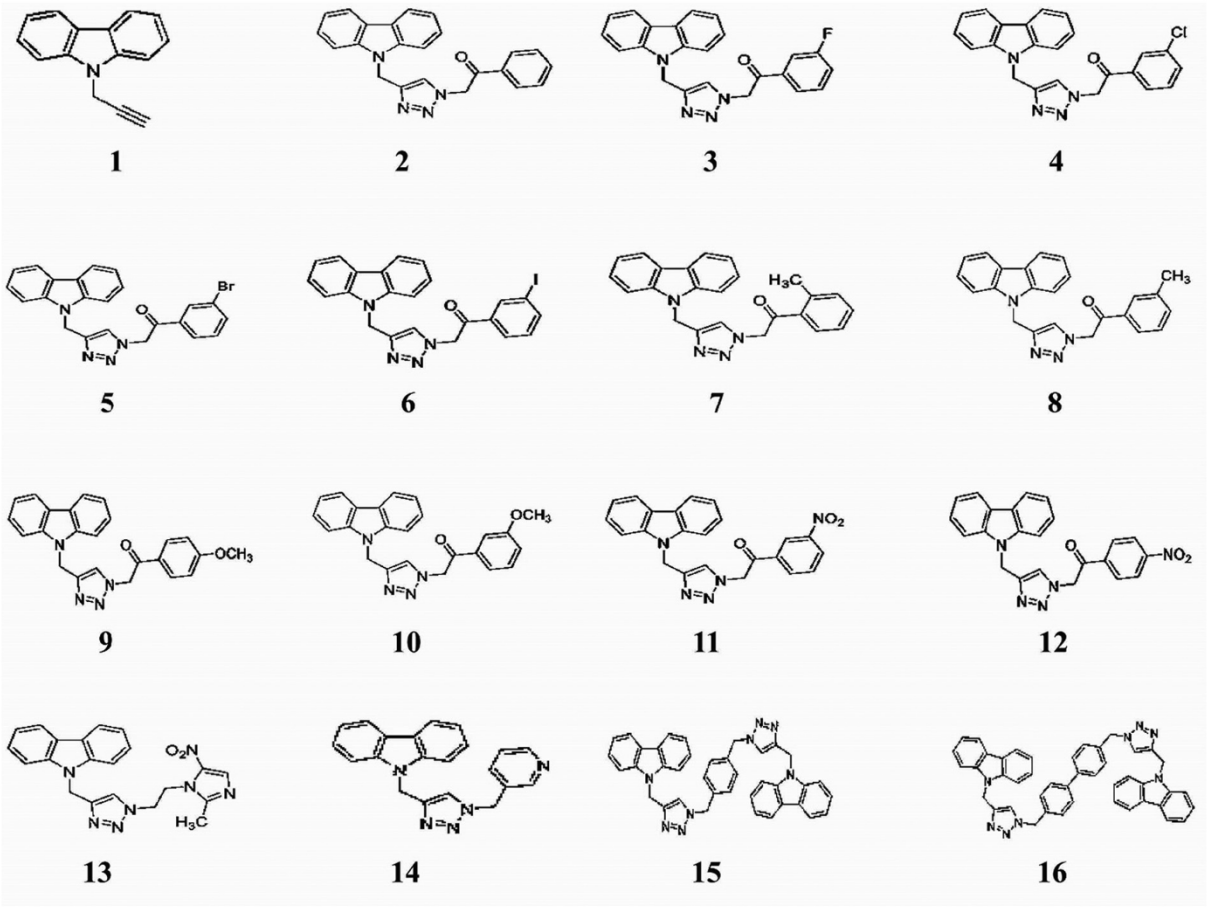

Fig. 2. Library of carbazole-1,2,3-triazole **2–16**.

presence of methoxy group, instead of methyl, at C-3 (compound **9**), and C-4 (compound **10**) positions causes a loss of antiglycation activity in both models.

Next, nitro substitution at C-3 (compound **11**) showed a moderate inhibition in both models (glucose-AGEs: $IC_{50} = 125 \pm 5.0$ μM, and MGO-AGEs: $IC_{50} = 147 \pm 10$ μM), as compared to references (rutin, and quercetin). To identify the substitution pattern that maximizes its antiglycation potential, a regioisomer of compound **11**, *i.e.*, compound **12** that possessed nitro group at the C-4 position was tested. Again, remarkable change in inhibitory activity was observed against glucose- and MGO- modified BSA with $IC_{50} = 69.8 \pm 2.4$ μM, and 76.1 ± 6.0 μM, respectively (See Table 1) than the reference molecules (rutin and quercetin).

Furthermore, compound **13**, possessing a pyridyl substitution at C-3 showed an excellent antiglycation activity in both models (glucose-AGEs: $IC_{50} = 63 \pm 3.0$ μM, and MGO-AGEs: 135 ± 5.0 μM). Moreover, compound **13** showed several fold better inhibition of protein glycation than the reference compounds in glucose-and MGO-AGEs model, while it showed similar inhibitory activity as the reference compound, quercetin. Compound **14** that possesses nitro imidazole at C-5 has shown a relatively lower activity against glucose-BSA model ($IC_{50} = 250 \pm 5.0$ μM), while it was inactive in MGO-BSA model.

Besides these, dimer of carbazole triazole (compound **15**) having phenyl ring, sandwiched between two carbazole linked 1,2,3-triazoles was also tested. Compound **15** has shown a moderate activity in both models (glucose-AGEs: $IC_{50} = 138 \pm 2.0$ μM, and MGO-AGEs: 333 ± 0.2 μM). Compound **16**, another dimer with biphenyl ring instead of phenyl, was tested and it showed a weak inhibition with $IC_{50} = 600 \pm 10.0$ μM in glucose-BSA model, while inactive in MGO-BSA model.

Table 1
Antiglycating activity of carbazole - traizole derivatives in glucose- and MGO-AGEs models.

Compounds	Glucose-AGEs		MGO-AGEs	
	% Inhibition ± SD[b]	IC_{50} [a] ± SD[b] (μM)	% Inhibition ± SD	IC_{50} [a] ± SD[b] (μM)
Rutin [s]	96.9 ± 0.1	83.9 ± 1.0	67.1 ± 2.1	104 ± 2.0
Quercetin [s]	88.8 ± 1.3	96.0 ± 4.0	58.7 ± 0.1	138.3 ± 4.4
1	60.9 ± 0.8	763.3 ± 15.2	26.6 ± 2.0	N_A^c
2	71.0 ± 0.5	351.3 ± 7.09	58.3 ± 1.5	797 ± 7.0
3	26.7 ± 4.7	N_A^c	18.2 ± 1.3	N_A^c
4	25.5 ± 5.04	N_A^c	15.6 ± 3.8	N_A^c
5	29.0 ± 6.98	N_A^c	22.1 ± 1.6	N_A^c
6	43.7 ± 3.14	N_A^c	39.5 ± 0.7	N_A^c
7	79.2 ± 1.05	180.3 ± 1.52	72.0 ± 1.2	275 ± 5.0
8	92.7 ± 1.5	65 ± 10.0	79 ± 1.15	130 ± 5.0
9	41.5 ± 4.2	N_A^c	18.1 ± 1.01	N_A^c
10	34.8 ± 7.4	N_A^c	12.1 ± 2.70	N_A^c
11	86.9 ± 0.6	125 ± 5.0	75.7 ± 0.95	147 ± 10
12	89.1 ± 0.8	69.8 ± 2.4	83.7 ± 0.71	76.1 ± 6.0
13	95.0 ± 0.36	63 ± 3.0	77.8 ± 0.53	135 ± 5.0
14	74.1 ± 1.52	250 ± 5.0	43.9 ± 0.76	N_A^c
15	79.0 ± 1.92	138 ± 2.0	71.8 ± 0.98	333 ± 0.2
16	65.8 ± 2.49	600 ± 10.0	41.5 ± 3.0	N_A^c

IC_{50}^a: Half minimum inhibitory concentration.
SD^b: Standard deviation.
N_A^c: Non-active.
Rutin[s], Quercetin[s]: Standard antiglycating agents.

3.2. Carbazole- linked 1,2,3-triazoles cytotoxicity profile in human HepG2 hepatocytes and THP-1 monocytes

To achieve our objectives, the toxicity of compounds was evaluated on liver hepatocytes and monocytes. It is well known that drugs withdrawal from clinical trials are often due to drug-induced hepatotoxicity. In the current study, the toxicity of test compounds was evaluated on hepatocytes as liver plays a major role in metabolic transformation of drug. Therefore, testing the toxicity of compounds on hepatocytes, in the early discovery phase, is an appropriate approach to assess the toxicological and pharmacological status of potential drug. Moreover, the cellular-based model for toxicological assessment is effective and economical than an experimental animal model [43].

Because compounds **1**–**2**, **7**–**8**, and **11**–**16** of carbazole-linked 1,2,3-triazoles, and parent carbazole (compound **1**) exhibited the antiglycation activity, they were tested for cytotoxicity at different concentrations (10–500 μM) in human HepG2 hepatocytes and THP-1 monocytes by using MTT and WST-1 metabolic assays, respectively. Rutin, and quercetin, as reference glycation inhibitors, and doxorubicin, as reference toxic compound, were used to compare the toxicity profile of different compounds. We found no toxic activity of **1**–**2**, **11**–**13**, and **15** up to 100 μM concentration either in human THP-1 monocytes or in HepG2 hepatocytes. Though they exhibited varying levels of cytotoxicity, from weak to moderate, at higher concentrations (250–500 μM), as reported in Fig. 3. Whereas, compounds **7**–**8**, **14**, and **16** showed toxicity in both THP-1 monocytes and HepG2 cell line. Percent viability of cells treated with standards and compounds at each tested concentration is presented in Supplementary Fig. 1a-c.

Therefore, the non-toxic compounds **1**–**2**, **11**–**13**, and **15** were selected to study their effect in reverting AGE-RAGE-induced intracellular ROS generation, increase of COX-2, and pro-inflammatory mediators in THP-1 monocytes.

The non-toxic concentration of both glucose- and MGO-AGEs was selected by assessing their effect on the viability of THP-1 monocytes at different concentrations (10, 30, 50, 100, 200, and 500 μg/mL). We found that the cell viability was not affected at 50 μg/mL of both glucose- and MGO-AGEs, therefore, 50 μg/mL AGEs were selected to study the effect of compounds against AGEs-induced ROS/NF-κB signaling, and increasing COX-2 protein and PGE_2 levels in monocytes (see Supplementary Fig. 2).

3.3. Carbazole- linked 1,2,3-triazoles impede glucose- and MGO- AGEs-induced oxidative stress in human THP-1 monocytes

In chronic hyperglycemia, glycated proteins exacerbate oxidative stress by generating ROS, resulting in pathophysiological effects on vascular system [7,22,45]. Our earlier study has highlighted the pathogenic role of AGEs through modulation of intracellular redox state in macrophages through RAGE/TLR4 nexus that consequently cause diabetic vascular impairments [26]. In the current study, we investigated the role of carbazole-linked 1,2,3-triazole derivatives **2**, **11**–**13**, and **15**, and compound **1** in inhibiting the AGE-RAGE- induced intracellular ROS production in AGEs-treated THP-1 monocyte models. Our data revealed that AGEs significantly elevate the ROS formation in activated THP-1 monocytes, as compared to untreated- and BSA-treated monocytes controls, by showing *P*-value <0.05 (Fig. 4a). These findings were consistent with previously reported studies [26,32]. The results showed that compounds **11**–**13**, and **15** reversed the RAGE ligation- mediated ROS formation in AGEs-activated THP-1 monocytes, as compared to the reference compounds (rutin, and quercetin), and PDTC (NF-κB inhibitor). Among all the tested compounds, compounds **12**, and **13** significantly inhibited the ROS formation, as much as PDTC and rutin in glucose-AGEs- treated THP-1 monocyte model. Compounds **2**, **11**, **15**, and quercetin exhibited a slightly lower antioxidant activity than compounds **12**, and **13** (Fig. 4).

Finally, compounds **12**, and **13** exhibited a potent antioxidant activity in MGO-AGEs-treated THP-1 monocyte model. They significantly ($P < 0.05$) suppressed the ROS formation, as inferred from green fluorescence intensity, in comparison to rutin. As shown in Fig. 4c, a slightly decreased inhibition was produced by compounds **2** and **11**, as compared to standards PDTC and quercetin. Based on the antiglycation and anti-oxidant activities, as well as on the nontoxic profile of carbazole-linked 1,2,3-triazole derivatives, compounds **12** and **13** were selected to study their possible inhibition of NF-κB activation. Parallel evaluation of COX-2 induction and PGE_2 production was carried out in AGE_S-activated THP-1 monocytes. ROS inhibition produced by reference molecules and tested compounds at each concentration in glucose- and MGO-AGEs models are presented in Supplementary Fig. 3a-d.

3.4. Carbazole- linked 1,2,3-triazoles suppress glucose- and MGO- AGEs-induced NF-κB translocation

Compounds **12**, and **13** role was further investigated in AGE-RAGE ligation-mediated NF-κB translocation *via* immunocytochemistry of p65 subunit. These compounds showed a potent antioxidant activity at the cellular level among all the tested carbazole-linked 1,2,3-triazole analogs. In agreement with previous study of Shanmugam, *et al* [22], we found that AGEs caused NF-κB translocation in THP-1 monocytes, comparable to BSA-treated THP-1 monocyte control model. The pretreatment of THP-1 monocytes with compounds **12**, and **13** significantly

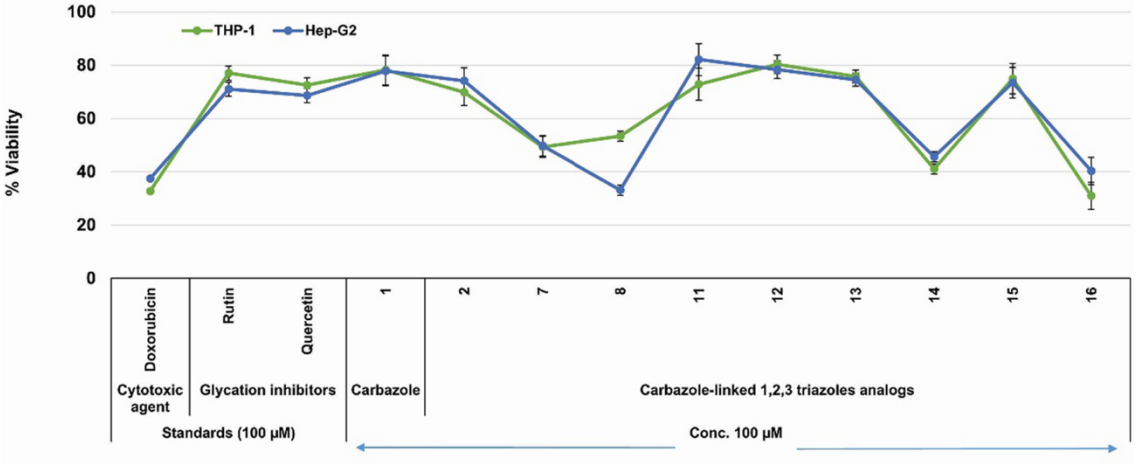

Fig. 3. Toxicity analysis of standards and selected carbazole- linked triazoles **1**–**2**, **7**–**8**, and **11**–**16** at 100 μM against human THP-1 monocytes, and HepG2 hepatocytes. Values of three independent experiments is presented as mean ± SD.

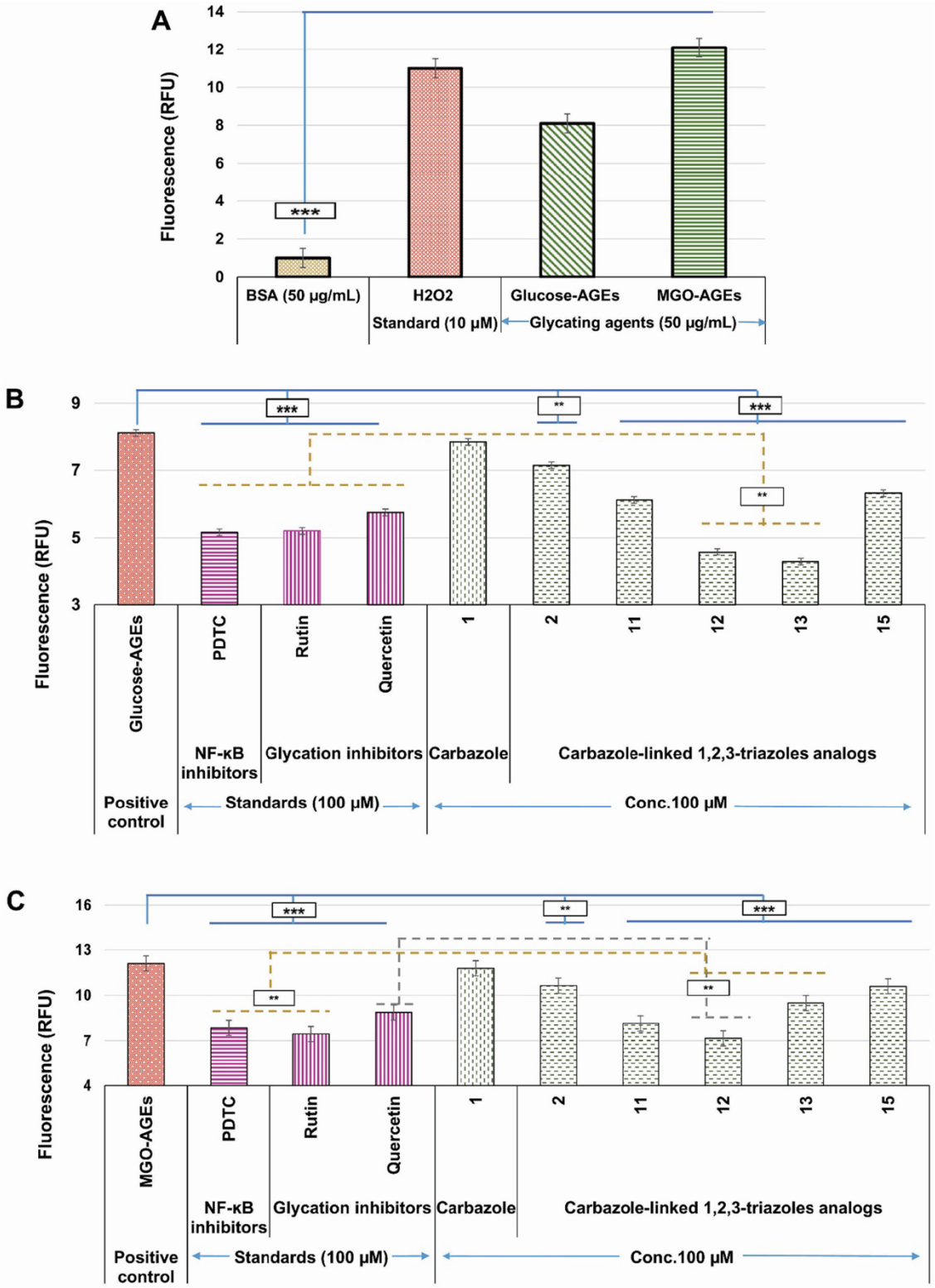

Fig. 4. AGE-RAGE ligation-induced intracellular ROS inhibition *via* selected carbazole-triazole analogs. (**A**) Briefly, the green fluorescence intensity in DCFH-DA probed human monocytes have found significantly increased at 485 nm excitation −520 nm emission, followed by the treatment of standard oxidizing (H_2O_2) and glycation agents (50 µg/mL; positive controls), as compared to BSA (negative control). (**B-C**) Cells pretreated with lead antiglycation compounds **2**, **11–13,** and **15**, and standards at 100 µM were significantly decreased ROS formation in glucose- and MGO-AGEs treated THP-1 models, respectively. Values of three independent experiments is presented as mean ± SD. *P* value <0.05, 0.01, and 0.001 are denoted by *, **, and *** respectively. (For interpretation of the references to colour in this figure legend, the reader is referred to the web version of this article.)

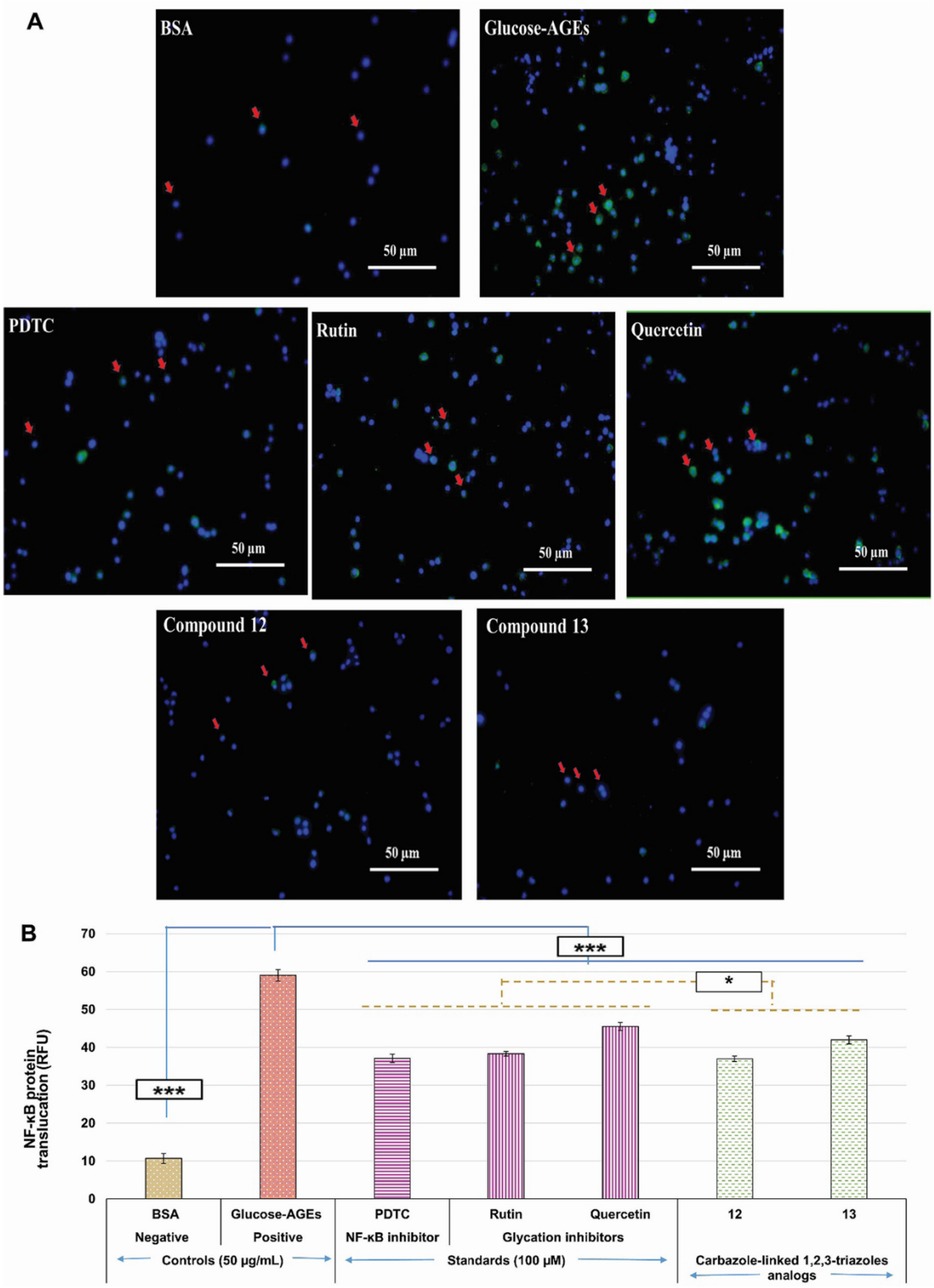

Fig. 5. Carbazole-1,2,3-triazole derivatives halt glucose-AGEs- induced NF-κB translocation in human monocytes model. (**A-B**) It is represented that glucose-AGEs at 50 µg/mL significantly increased NF-κB fluorescence, as compared to negative control (BSA), whereas, the green fluorescence was significantly reduced with compounds **12**, and **13** treatment. Value of three independent experiments is presented as mean ± SD. P value <0.05, 0.01, and 0.001 are denoted by by *, **, and *** respectively. (For interpretation of the references to colour in this figure legend, the reader is referred to the web version of this article.)

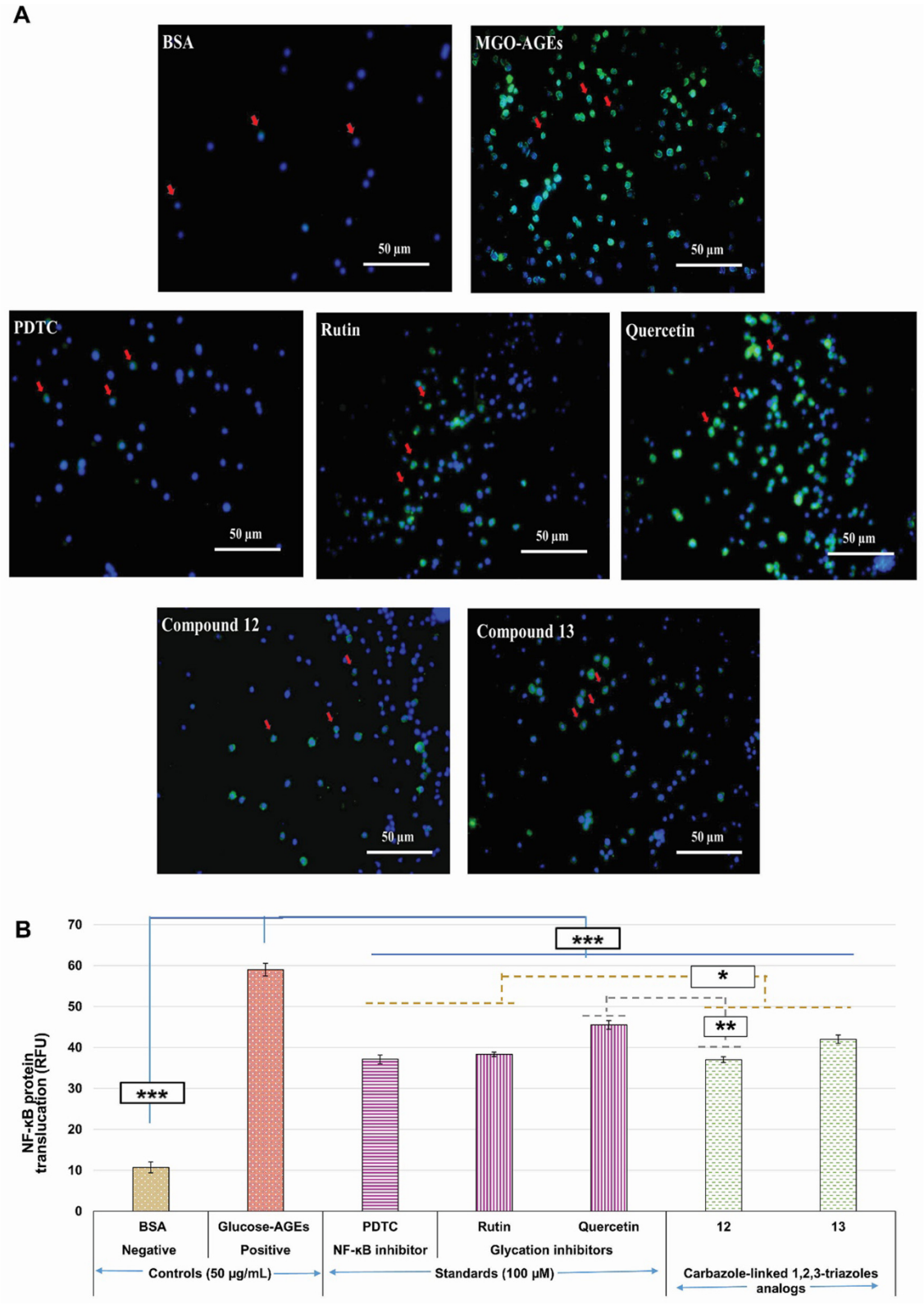

Fig. 6. Carbazole-1,2,3-triazole derivatives inhibit MGO-AGEs mediated NF-κB translocation in human monocytes model. (**A-B**) It is represented that MGO-AGEs (50 µg/mL) significantly increased NF-κB translocation, as compared to BSA (negative control). Pretreatment of cells with compounds **12**, and **13** reduced the intensity of green fluorescence by halting NF-κB translocation. Value of three independent experiments is presented as mean ± SD. P value <0.05, 0.01, and 0.001 are denoted by *, **, and *** respectively. (For interpretation of the references to colour in this figure legend, the reader is referred to the web version of this article.)

decreased the AGEs-treated NF-kβ translocation (*P*-value <0.05). Compounds **12**, and **13** were found to be more active than standards PDTC and rutin in both models. They expressed relatively higher suppressive potential of NF-κB translocation than standard quercetin in glucose-AGEs model, whereas compound **12** was found more potent than quercetin in MGO-AGEs model. Compound **13** exhibited similar activity as quercetin in MGO-AGEs model, as shown in Fig. 5a, and b, and 6a, and b. These observations suggest that the inhibitory effect of compounds **12**, and **13** on NF-κB translocation was associated with AGEs-induced ROS inhibition in THP-1 monocytes (See Supplementary Fig. 4a-d).

3.5. Carbazole-linked 1,2,3-triazoles reduce induction of glucose- and MGO-AGEs- induced proinflammatory COX-2

Based on promising inhibitory effect on RAGE ligation-mediated ROS/NF-κB, compounds **12**, and **13** were further studied for their ability to prevent elevated COX-2 protein levels in AGEs-activated THP-1 monocytes. The cells were pretreated with compounds **12**, and **13** at 100 μM for an hour, and then stimulated with AGEs for 6 h. Following protein extraction, western blotting and normalization with ß-actin protein were performed, and the levels of COX-2 were determined as fold inductions. Our results were consistent with the previously reported studies [22]. COX-2 levels were higher in AGEs-treated THP-1 monocyte than in BSA-treated control (*P*-value <0.05), as depicted in Fig. 7a. Compounds **12** and **13** produced 3- and 3.5-fold reduction of COX-2 (Fig. 7b), respectively. In MGO-AGEs-treated THP-1 model, the compounds **12**, and **13** produced 2.1-, and 1.34-fold decrease in COX2 levels, respectively (Fig. 7c). Our data revealed that compounds **12**, and **13** were more potent in decreasing COX-2 levels, induced by both AGEs, as compared to standards PDTC (glucose-AGEs: 2.16-fold; MGO-AGEs: 1.60-fold) and rutin (glucose-AGEs: 2.09-fold; MGO-AGEs: 1.65-fold). Compounds **12** and **13** exhibited a greater activity than quercetin (1.6-fold) in glucose-AGE-treated THP-1 monocytes. Compound **12** also exhibited a greater activity than quercetin (1.31-fold) in MGO-AGE-treated model, while compound **13** showed a similar activity as quercetin.

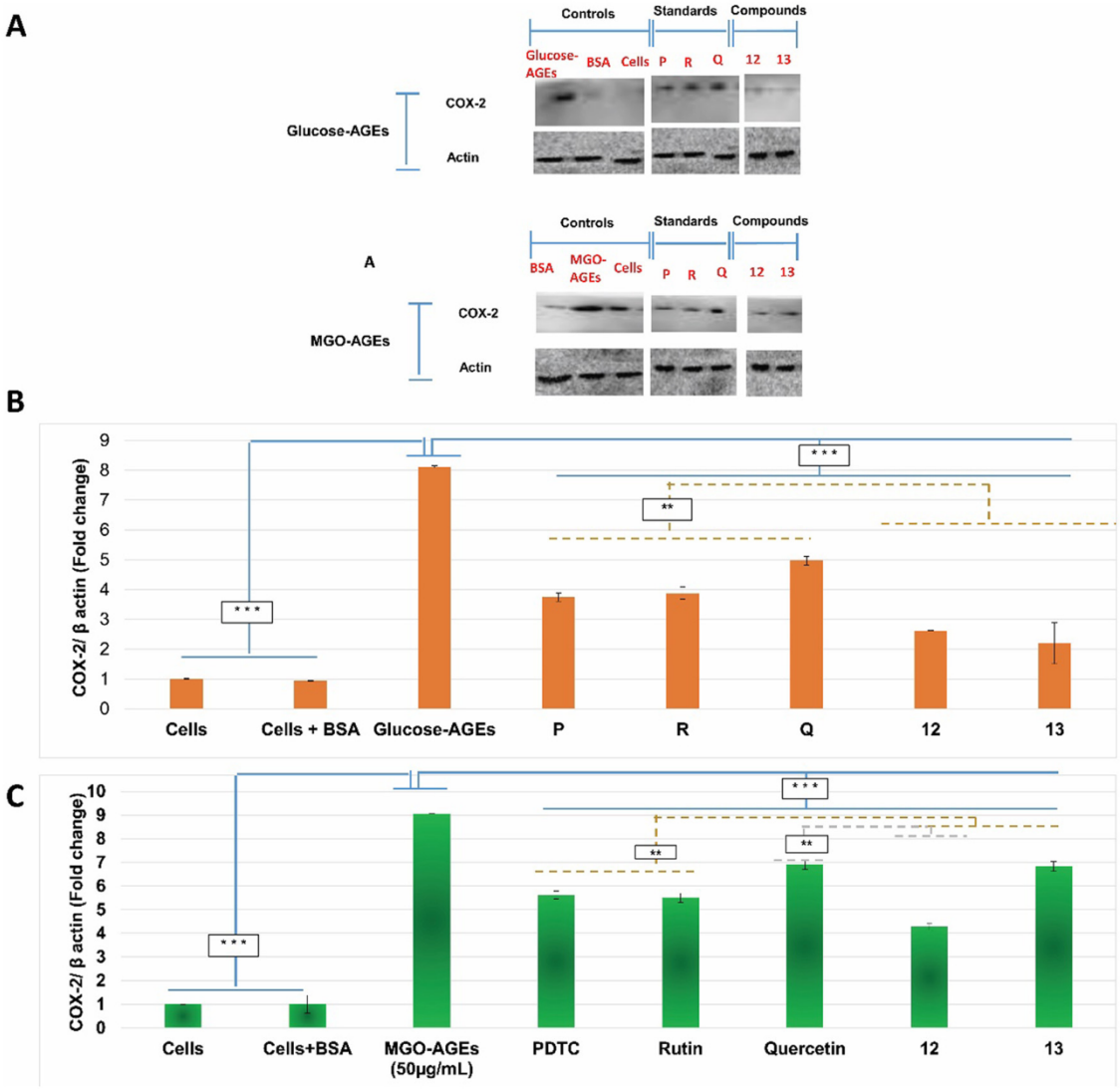

Fig. 7. Reduction of glucose- and MGO-AGEs-mediated COX-2 levels *via* selected carbazole-1,2,3-triazole analogs. (**A**) It is represented that human monocytes pretreated with compounds **12**, and **13** at 100 μM for an hour, and stimulated with glucose- and MGO-AGEs for 6 h significantly reduced the COX-2 protein expression. (**B**-**C**) The reduction in AGE-RAGE-mediated COX-2 levels were observed as fold change, as compared to control AGEs. ß-Actin was used as an internal reference to normalize COX-2 protein expression. Values of two independent experiments is presented as mean ± SD. P value <0.05, 0.01, and 0.001 are denoted by *, **, and *** respectively.
Abbreviations: P: PDTC, R: Rutin, Q: Quercetin.

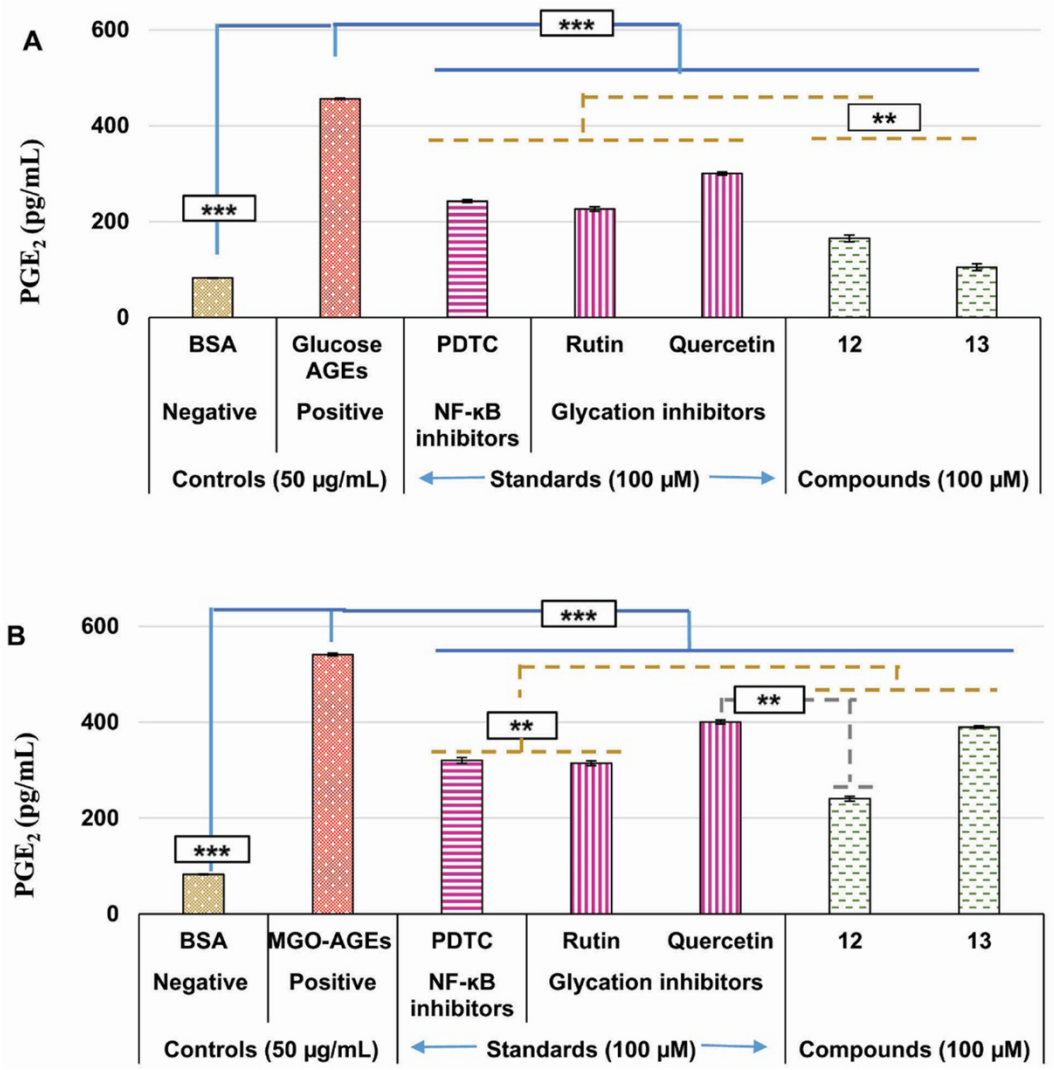

Fig. 8. Inhibition of AGEs-induced proinflammatory PGE_2 *via* carbazole-triazole analogs in monocytes models. (**A**-**B**) Cells pre-treated with standards (PDTC, rutin, quercetin), and compounds **12**, and **13** exhibited a significantly reduced AGEs-induced PGE_2 formation, as measured in cells supernatant by using ELISA. Values of two independent experiments is presented as mean ± SD. P value <0.05, 0.01, and 0.001 are denoted by *, **, and *** respectively.

3.6. Carbazole- linked 1,2,3-triazoles alleviate glucose- and MGO-AGEs-induced PGE_2 levels

AGEs induce the production of proinflammatory mediator PGE_2 *via* COX-2 upregulation, which is associated with complex diabetic vascular complications [22,32]. Considering the role of compounds **12**, and **13** in alleviating AGEs-mediated upregulation of COX-2, their inhibitory effect was investigated on PGE_2 production in THP-1 monocytes. Compounds **12**, and **13** significantly reduced the PGE_2 levels (P value <0.05) in AGEs-treated THP-1 monocytes, as shown in Fig. 8a, and b. PDTC and rutin exhibited a relatively greater suppression of PGE_2 levels in both glucose- and MGO-AGEs models than quercetin.

These findings suggest that compounds **12**, and **13** by interfering AGE-RAGE-ligation, can decrease ROS generation and NF-κB activation in human monocytes. Consequently, the levels of proinflammatory markers, such as COX-2, and PGE_2 decline. The present study identifies carbazole-linked 1,2,3-triazoles **12**, and **13** as potential downregulators of COX-2 protein *via* impeding AGEs-induced proinflammatory intracellular cascade.

4. Discussion

Chronic hyperglycemia accelerates the non-enzymatic protein glycation [4,33]. The non-enzymatic protein glycation involves methylglyoxal (MGO) as a highly reactive intermediate, which leads to the formation of AGEs [44]. AGE-RAGE ligation leads to the activation of intracellular inflammatory mediators, thereby it activates peripheral monocytes and induces vascular dysfunction [32,45]. In the present study, the MGO-BSA glycation model was employed by incubating BSA with MGO. The formation of MGO-BSA (dicarbonyl sugar containing AGEs) was quantified following 24 h of incubation, instead of 7 days incubation as in the classical glucose-BSA model (single carbonyl sugar containing AGEs) that we also used in comparison with MGO-BSA. Our data demonstrate that carbazole-linked 1,2,3-triazole analogs possess inhibitory activity in both glycation models.

The extent of inhibitory activity of test compounds was greatly influenced by the substitution pattern, and carbonyl moieties. The addition of acetophenone ring in carbazole-triazole skeleton has yielded a remarkable increase in the inhibition of protein glycation in both models. The compounds substituted with halogen moieties, such as fluoro (compound **3**), chloro (compound **4**), bromo (compound **5**), and iodo (compound **6**) at C-3 of acetophenone ring were found to be

inactive in both models. Whereas, methylation at C-2 (compound **7**) had exhibited a relatively moderate inhibition in both models, as compared to methyl group at C-3 position (compound **8**) which contributed substantially in *in vitro* antiglycation activity. Furthermore, the methoxy substitution at C-3, and C-4 (compounds **9**, and **10**), respectively resulted in a loss of activity in both models. Next, nitro moiety at C-3 (compound **11**) had shown a moderate inhibitory activity in both models, while substitution of nitro moiety at C-4 produced a remarkable outcome with an excellent inhibitory activity of compound **12** in both models. Furthermore, pyridine substitution at C-3 in compound **13** suppressed the protein glycation, whereas nitro imidazole substitution at C-5 in heterocyclic compound **14** showed a weak activity in glucose-BSA model, and no activity in MGO-BSA model.

At last, dimer of carbazole triazole (compound **15**) with phenyl ring between two carbazole-linked 1,2,3-triazole displayed a moderate antiglycation activity in both models. The dimer with biphenyl ring (compound **16**) further showed a decrease in activity in glucose-BSA model, but no activity in MGO-BSA model.

Carbazole-linked 1,2,3-triazoles exerted a preventive influence against AGEs-mediated dysfunction at cellular levels. We observed that in downstream inflammatory cascades initiated by AGE-RAGE interaction, the most active compounds **12**, and **13** actively reduced AGEs-mediated effects. Finally, we propose that nitro substitution at C-4 of acetophenone and C-3′ pyridyl substitution at the carbazole-1,2,3-triazoles skeleton in compounds **12**, and **13**, respectively, confer the compounds the inhibitory activity against AGEs-induced-inflammatory mediators.

Numerous studies highlighted the role of AGEs-RAGE ligation in oxidative imbalance and elevated pro-inflammatory mediators with activation of monocytes [32,45] and other cell types, including macrophages, neutrophils, eosinophils, and cardiomyocytes, [46,47]. The underlying mechanisms involve the activation of NADPH oxidase (NOX) with stimulation of both the mitochondrial respiratory chain complex [48] and NF-κB pathway [49]. Several studies have reported disproportion from the baseline levels of endogenous pro-oxidative and anti-oxidative enzymes, resulting in ROS formation. The overwhelming intracellular oxidative stress ilead to the on-set of diabetic vascular complications [50,51]. ROS is one of the prominent players in AGEs-stimulated pro-inflammatory pathway, associated with NF-κB activation [32,52]. In line with that evidence, the present study reports an increase in ROS generation in THP-1 monocytes in response of AGEs treatment. Carbazole-linked 1,2,3-triazoles **12**, and **13** pretreatment has caused a reduction in ROS formation, as reference antiglycation agents. Our findings are consistent with the study by Shazia *et al.,* that demonstrated ROS inhibition *via* bicarbazole-linked triazoles in human whole blood and isolated neutrophils abated inflammation [53].

Previous studies indicated that AGE-RAGE-ligation-mediated intracellular ROS production stimulates NF-κB in diabetes [22,26,54]. The AGE-RAGE ligation is associated with *de novo* RelA(p65) mRNA synthesis, which persistently accumulates transcriptionally active NF-κB [55]. Similarly, our study shows that the increase ROS formation causes the activation of NF-κB, following treatment of THP-1 monocytes with AGEs. Besides, monocytes pretreatment with PDTC, a standard NF-κB inhibitor, has inhibited RAGE-ligation induced ROS / NF-κB in cells. The treatment with carbazole-linked 1,2,3-triazoles **12**, and **13** also attenuated the glucose- and MGO-AGEs-induced NF-κB (p65) translocation in human THP-1 monocytes. This suggests that compounds **12**, and **13** can suppress the NF-κB mediated signaling by partly interfering with the AGE-RAGE/ROS nexus in monocytes.

Increasing body of evidence supports the role of COX-2 in the pathophysiology of atherosclerosis [22,23]. The COX-2 upregulation increases inflammatory mediators that initiate vascular monocyte adhesion and migration, and hence cause chronic vascular inflammation [56 –57]. AGE-RAGE interaction is associated with accelerated inflammatory response by the upregulation of COX-2 expression, and associated PGE_2 secretion in monocytes [58,59], thereby playing a role in diabetes-associated vascular dysfunction [22,32]. Growing evidence points out the relevance of COX-2 inhibition as therapeutic approaches to avert atheroma formation [22,32,50]. Our findings also establish that AGEs treatment elevates COX-2 protein and PGE_2 levels by activating ROS/NF-κB signaling in the monocytes. Compounds **12**, and **13** pretreatment effectively suppress the AGEs-induced COX-2 and PGE_2 levels in THP-1 monocytes. Our findings are in agreement with the study of Feng-Ming Ho *et al.* [60]. They reported that LCY-2-CHO (carbazole derivative) downregulates proinflammatory iNOS, COX-2, and TNF-α gene expression *via* inhibiting the p38 MAPK pathway, and AP-1 activation in macrophages [60]. Our findings are also in-line with the earlier study of Taechowisan *et al.* that showed that 3- methylcarbazoles (carbazole derivative) suppressed proinflammatory PGE_2 in LPS- and pam3CSK-activated macrophages, and thus prevented inflammation [61]. Moreover, the MAP kinases (extracellular signal-regulated kinase and c-Jun N-terminal kinase), and NF-κB nexus are components of the AGE-RAGE intracellular cascade and regulate COX-2 expression in monocytes [59,62]. The present study further supports our findings about the role of AGE-RAGE/ NF-κB nexus in COX-2 induction, and inhibition *via* PDTC (NF-κB nexus inhibitor) and carbazole-linked triazoles.

5. Conclusion

Novel carbazole-linked 1,2,3-triazole derivatives, carrying a nitro substitution at C-4 of acetophenone or a 3′ pyridyl substitution at the ring of carbazole-1,2,3-triazoles skeleton, have shown to inhibit both the *in vitro* formation of AGEs and their pro-inflammatory effect on THP-1 monocytes. By interfering with the protein glycation reaction, these compounds were found as novel antiglycation agents with a potential to prevent or delay the onset of vascular inflammation in diabetes. The validation of this preliminary results towards the treatment of vascular diabetic disease deserves further investigation in *in vivo* animal model.

Credit authorship contribution statement

Humera Jahan: Conceptualization, Data curation, Funding acquisition, Formal analysis, Investigation, Methodology, Project administration, Resources, Supervision, Writing - original draft, Writing - review & editing, Visualization. **M. Iqbal Choudhary**: Conceptualization, Formal analysis, Resources, Supervision, and Writing - review & editing. **Nimra Naz Siddiqui:** Methodology, Investigation, Writing - original draft. **Shazia Iqbal:** Synthesis of compounds. **Sadia Shaikh:** Methodology. **Fatima Z. Basha:** Supervision of synthesis. **Marina Pizzi:** Review.

Data availability statement

The data that support the findings of this study are available from the corresponding author upon request. Some data may not be made available because of privacy or ethical restrictions.

Declaration of Competing Interest

The authors declare that they have no known competing financial interests or personal relationships that could have appeared to influence the work reported in this paper.

Acknowledgements

This work was supported by the Higher Education Commission (Grant No: 20-GCF-1044/RGM/R&ID/HEC/2021), and the World Academy of Sciences (TWAS-COMSTECH Research Grant Award_17-295 RG/PHA/AS_C).

Appendix A. Supplementary data

Supplementary data to this article can be found online at https://doi.org/10.1016/j.cellsig.2022.110372.

References

[1] M. Bode, N. Mackman, Regulation of tissue factor gene expression in monocytes and endothelial cells: thromboxane A2 as a new player, Vasc. Pharmacol. 62 (2) (2014) 57–62.
[2] M. Kitada, et al., Molecular mechanisms of diabetic vascular complications, J. Diab. Investig. 1 (3) (2010) 77–89.
[3] S. Yamagishi, T. Imaizumi, Diabetic vascular complications: pathophysiology, biochemical basis and potential therapeutic strategy, Curr. Pharm. Des. 11 (18) (2005) 2279–2299.
[4] H Jahan, M.I. Choudhary, Glycation, carbonyl stress and AGEs inhibitors: a patent review, Exp. Opin. Ther. Pat. 25 (11) (2015) 1267–1284.
[5] A.M. Schmidt, et al., Activation of receptor for advanced glycation end products: a mechanism for chronic vascular dysfunction in diabetic vasculopathy and atherosclerosis, Circ. Res. 84 (5) (1999) 489–497.
[6] Z.A. Khan, S. Chakrabarti, Cellular signaling and potential new treatment targets in diabetic retinopathy, Exp. Diabetes Res. 2007 (2007) 31867.
[7] H. Jahan, et al., Insulinotropic action of 2, 4-dinitroanilino-benzoic acid through the attenuation of pancreatic beta-cell lesions in diabetic rats, Chem. Biol. Interact. 273 (2017) 237–244.
[8] C. Rask-Madsen, G.L. King, Vascular complications of diabetes: mechanisms of injury and protective factors, Cell Metab. 17 (1) (2013) 20–33.
[9] Y.K. Chuah, et al., Receptor for advanced Glycation end products and its involvement in inflammatory diseases, Int. J. Inflamm. 2013 (2013), 403460.
[10] A. Bierhaus, et al., Advanced glycation end product-induced activation of NF-κB is suppressed by alpha-lipoic acid in cultured endothelial cells, Diabetes 46 (9) (1997) 1481–1490.
[11] A. Bustami, et al., The anti-inflammatory effect of octyl gallate through inhibition of nuclear factor-κB (NF-κB) pathway in rat endometriosis model, J. Reprod. Infertil. 21 (3) (2020) 169–175.
[12] N. Jangde, R. Ray, V. Rai, RAGE and its ligands: from pathogenesis to therapeutics, Crit. Rev. Biochem. Mol. Biol. 55 (6) (2020) 555–575.
[13] A. Speciale, et al., Anthocyanins as modulators of cell redox-dependent pathways in non-communicable diseases, Curr. Med. Chem. 27 (12) (2020) 1955–1996.
[14] T.V. Kirichenko, et al., Medicinal plants as a potential and successful treatment option in the context of atherosclerosis, Front. Pharmacol. 11 (2020) 403.
[15] F. Cipollone, B. Rocca, C. Patrono, Cyclooxygenase-2 expression and inhibition in atherothrombosis, Arterioscler. Thromb. Vasc. Biol. 24 (2) (2004) 246–255.
[16] C.K. Glass, J.L. Witztum, Atherosclerosis. The road ahead, Cell 104 (4) (2001) 503–516.
[17] C.L. Fisher, S.L. Demel, Nonsteroidal anti-inflammatory drugs: a potential pharmacological treatment for intracranial aneurysm, Cerebrovasc. Diseas. Extra 9 (1) (2019) 31–45.
[18] P.P. Rao, S.N. Kabir, T. Mohamed, Nonsteroidal anti-inflammatory drugs (NSAIDs): progress in small molecule drug development, Pharmaceuticals 3 (5) (2010) 1530–1549.
[19] S. Bindu, S. Mazumder, U. Bandyopadhyay, Non-steroidal anti-inflammatory drugs (NSAIDs) and organ damage: a current perspective, Biochem. Pharmacol. 180 (2020), 114147.
[20] R.C. Harris, M.D. Breyer, Update on cyclooxygenase-2 inhibitors, Clin. J. Am. Soc. Nephrol. 1 (2) (2006) 236–245.
[21] R. Kharb, P.C. Sharma, M.S. Yar, Pharmacological significance of triazole scaffold, J. Enzyme Inhibit. Med. Chem. 26 (1) (2011) 1–21.
[22] N. Shanmugam, et al., Regulation of cyclooxygenase-2 expression in monocytes by ligation of the receptor for advanced glycation end products, J. Biol. Chem. 278 (37) (2003) 34834–34844.
[23] S. Yamagishi, T. Matsui, Advanced glycation end products, oxidative stress and diabetic nephropathy, Oxidative Med. Cell. Longev. 3 (2) (2010) 101–108.
[24] R. Nagai, et al., Chelation: a fundamental mechanism of action of AGE inhibitors, AGE breakers, and other inhibitors of diabetes complications, Diabetes 61 (3) (2012) 549–559.
[25] S.K. Venugopal, et al., Alpha-tocopherol decreases superoxide anion release in human monocytes under hyperglycemic conditions via inhibition of protein kinase C-alpha, Diabetes 51 (10) (2002) 3049–3054.
[26] H. Jahan, M.I. Choudhary, Gliclazide alters macrophages polarization state in diabetic atherosclerosis in vitro via blocking AGE-RAGE/TLR4-reactive oxygen species-activated NF-κB nexus, Eur. J. Pharmacol. 894 (2021), 173874.
[27] S. Issa, et al., Carbazole scaffolds in cancer therapy: a review from 2012 to 2018, J. Enzyme Inhibit. Med. Chem. 34 (1) (2019) 1321–1346.
[28] H. Li, R. Aneja, I. Chaiken, Click chemistry in peptide-based drug design, Molecules 18 (8) (2013) 9797–9817.
[29] R. Kharb, P.C. Sharma, M.S. Yar, Pharmacological significance of triazole scaffold, J. Enzyme Inhib. Med. Chem. 26 (1) (2011) 1–21.
[30] M.R. Dasu, S. Devaraj, I. Jialal, High glucose induces IL-1beta expression in human monocytes: mechanistic insights, Am. J. Physiol. Endocrinol. Metab. 293 (1) (2007) E337–E346.
[31] S.K. Venugopal, et al., α-Tocopherol decreases superoxide anion release in human monocytes under hyperglycemic conditions via inhibition of protein kinase C-α, Diabetes 51 (10) (2002) 3049–3054.
[32] C.H. Wu, et al., Naturally occurring flavonoids attenuate high glucose-induced expression of proinflammatory cytokines in human monocytic THP-1 cells, Mol. Nutr. Food Res. 53 (8) (2009) 984–995.
[33] H. Jahan, et al., Inhibitors of advanced glycation end-products (ages) formation, 2016. US 9387198.B1 Patents.
[34] L. Cabrol, M. Quéméneur, B. Misson, Inhibitory effects of sodium azide on microbial growth in experimental resuspension of marine sediment, J. Microbiol. Methods 133 (2017) 62–65.
[35] J.H. Heo, et al., Acetylcholinesterase and butyrylcholinesterase inhibitory activities of khellactone coumarin derivatives isolated from Peucedanum japonicum Thurnberg, Sci. Rep. 10 (1) (2020) 1–11, 21695.
[36] A. Balakrishna, M.H. Kumar, Evaluation of synergetic anticancer activity of Berberine and Curcumin on different models of A549, Hep-G2, MCF-7, Jurkat, and K562 cell lines, Biomed. Res. Int. 2015 (2015), 354614.
[37] Q. Jiang, et al., Combined effects of low levels of palmitate on toxicity of ZnO nanoparticles to THP-1 macrophages, Environ. Toxicol. Pharmacol. 48 (2016) 103–109.
[38] J.D. McPherson, B.H. Shilton, D.J. Walton, Role of fructose in glycation and cross-linking of proteins, Biochemistry 27 (6) (1988) 1901–1907.
[39] Y. Hu, et al., Mitochondrial pathway is involved in advanced glycation end products-induced apoptosis of rabbit annulus fibrosus cells, Spine 44 (10) (2019) E585.
[40] K.-F. Liao, et al., Etodolac and the risk of acute pancreatitis, Biomedicine 7 (1) (2017).
[41] G.N. Kim, H.D. Jang, Protective mechanism of quercetin and rutin using glutathione metabolism on HO-induced oxidative stress in HepG2 cells, Ann. N. Y. Acad. Sci. 117191 (1) (2009) 530–537.
[42] C.H. Wu, G.C. Yen, Inhibitory effect of naturally occurring flavonoids on the formation of advanced glycation endproducts, J. Agric. Food Chem. 53 (8) (2005) 3167–3173.
[43] K.N. Prasad, Oxidative stress, pro-inflammatory cytokines, and antioxidants regulate expression levels of MicroRNAs in Parkinson's disease, Curr. Aging Sci. 10 (3) (2017) 177–184.
[44] C. Nevin, et al., Investigating the Glycating effects of glucose, Glyoxal and Methylglyoxal on human sperm, Sci. Rep. 8 (1) (2018) 1–12.
[45] S. Costantino, F. Paneni, F. Cosentino, Hyperglycemia: a bad signature on the vascular system, Cardiovasc. Diagn. Ther. 5 (5) (2015) 403–406.
[46] K. Kierdorf, G. Fritz, RAGE regulation and signaling in inflammation and beyond, J. Leukoc. Biol. 94 (1) (2013) 55–68.
[47] G. Daffu, et al., Radical roles for RAGE in the pathogenesis of oxidative stress in cardiovascular diseases and beyond, Int. J. Mol. Sci. 14 (10) (2013) 19891–19910.
[48] A. Tarafdar, G. Pula, The role of NADPH oxidases and oxidative stress in neurodegenerative disorders, Int. J. Mol. Sci. 19 (12) (2018).
[49] W. Cai, et al., AGER1 regulates endothelial cell NADPH oxidase-dependent oxidant stress via PKC-δ: implications for vascular disease, Am. J. Phys. Cell Phys. 298 (3) (2010) C624–C634.
[50] D. Pitocco, et al., Oxidative stress in diabetes: implications for vascular and other complications, Int. J. Mol. Sci. 14 (11) (2013) 21525–21550.
[51] T. Nishikawa, et al., Impact of mitochondrial ROS production on diabetic vascular complications, Diabetes Res. Clin. Pract. 77 (3) (2007) S41–S45.
[52] X. Yan, et al., Nuclear factor kappa B activation and regulation of cyclooxygenase type-2 expression in human amnion mesenchymal cells by interleukin-1beta, Biol. Reprod. 66 (6) (2002) 1667–1671.
[53] S. Iqbal, et al., Synthesis of new bicarbazole-linked triazoles as non-cytotoxic reactive oxygen species (ROS) inhibitors, Synth. Commun. 49 (18) (2019) 2330–2341.
[54] H. Jahan, et al., Derivatives of 6-Nitrobenzimidazole inhibit fructose-mediated protein Glycation and intracellular reactive oxygen species production, Med. Chem. 13 (6) (2017) 577–584.
[55] A. Bierhaus, et al., Diabetes-associated sustained activation of the transcription factor nuclear factor-kappaB, Diabetes 50 (12) (2001) 2792–2808.
[56] R. Nørregaard, T.-H. Kwon, J. Frøkiær, Physiology and pathophysiology of cyclooxygenase-2 and prostaglandin E2 in the kidney, Kidney Res. Clin. Pract. 34 (4) (2015) 194–200.
[57] L. Shi, et al., Liraglutide attenuates high glucose-induced abnormal cell migration, proliferation, and apoptosis of vascular smooth muscle cells by activating the GLP-1 receptor, and inhibiting ERK1/2 and PI3K/Akt signaling pathways, Cardiovasc. Diabetol. 14 (1) (2015) 1–13.
[58] M.F. Linton, S. Fazio, Cyclooxygenase-2 and inflammation in atherosclerosis, Curr. Opin. Pharmacol. 4 (2) (2004) 116–123.
[59] H. Jahan, et al., Indole-linked 1, 2, 3-triazole derivatives efficiently modulate COX-2 protein levels in human THP-1 monocytes by suppressing AGE-ROS-NF-kβ nexus, Life Sci. 291 (2022) 120282.
[60] F.-M. Ho, et al., The anti-inflammatory carbazole, LCY-2-CHO, inhibits lipopolysaccharide-induced inflammatory mediator expression through inhibition of the p38 mitogen-activated protein kinase signaling pathway in macrophages, Br. J. Pharmacol. 141 (6) (2004) 1037–1047.
[61] T. Taechowisan, et al., Anti-inflammatory effect of 3-methylcarbazoles on RAW 264.7 cells stimulated with LPS, polyinosinic-polycytidylic acid and Pam3CSK, Adv. Microbiol. 2 (2) (2012) 98–103.
[62] P. Younessi, A. Yoonessi, Advanced glycation end-products and their receptor-mediated roles: inflammation and oxidative stress, Iran. J. Med. Sci. 36 (3) (2011) 154–166.